The 3-Meter Dish at the "Astropeiler Stockert"

Part 2: Characterisation and Observations

Wolfgang Herrmann

1. Introduction

In part 1 of the articles about the 3-m dish we have described the setup. This part will now deal with the characterisation of the instrument and the observations.

2. First Light

First light with this telescope was achieved on July 28th, 2017. At that time, the telescope was not fully completed yet. However, it could be moved, feed horn and LNA were mounted and some preliminary equipment could be used for testing.
The first test was to look for the increase in noise when pointing towards the Sun. We found that we had an increase of 9 dB at 1420 MHz. This encouraged us to also look for some hydrogen spectrum. Since we did not have the means yet to point the telescope towards a specific astronomical source, we had to make a rough guess on where the galactic plane would be. We moved the telescope in that direction and took a spectrum.
The result is shown below in fig. 1. We consider this to be our official “first light”.

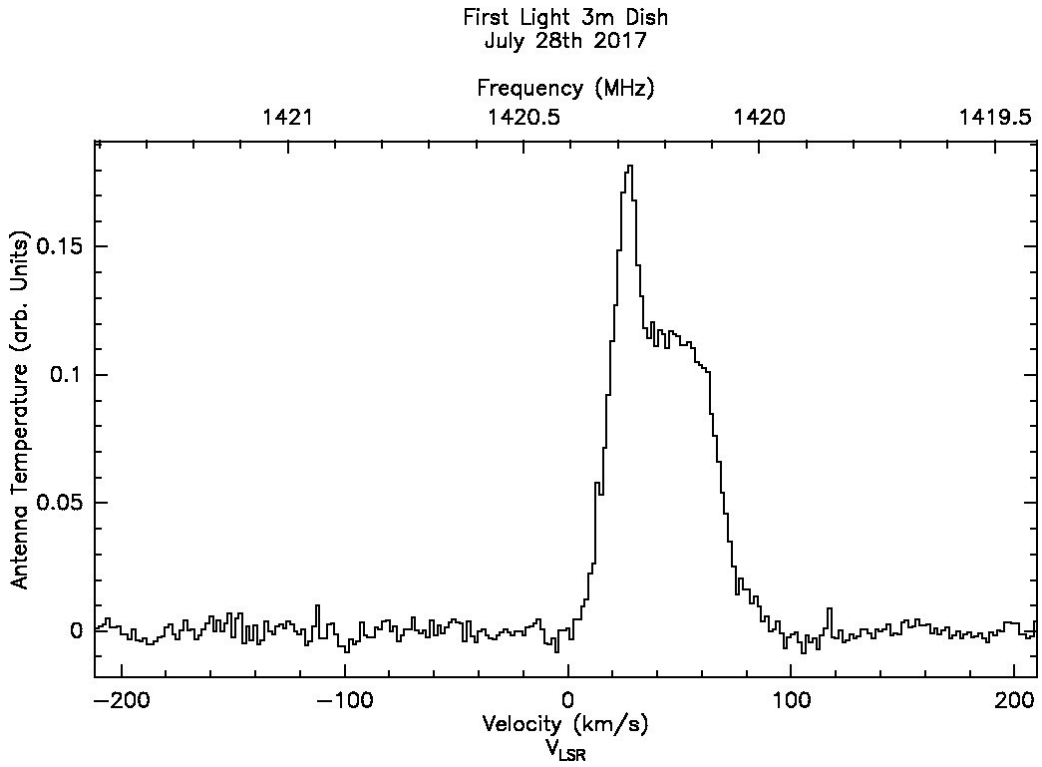

Figure 1: *First Light of the 3-meter telescope: Hydrogen spectrum*

3. Characteristics

Once the setup was finalized, various parameters of the telescope have been determined in order to fully understand its characteristics and to check whether the performance meets the expectations.

3.1. Beam width and side lobes

The full width half maximum beam width W of an ideally illuminated parabolic dish is

$$W = arcsin\left(1.22\frac{\lambda}{D}\right) \qquad (1)$$

where λ is the wavelength and D the diameter of the dish. At 21 cm and a dish of 3-meter diameter this would be about 4.9°. In fig. 2 below the measured beam profile is shown. This measurement has been done via a transit scan of the Sun.

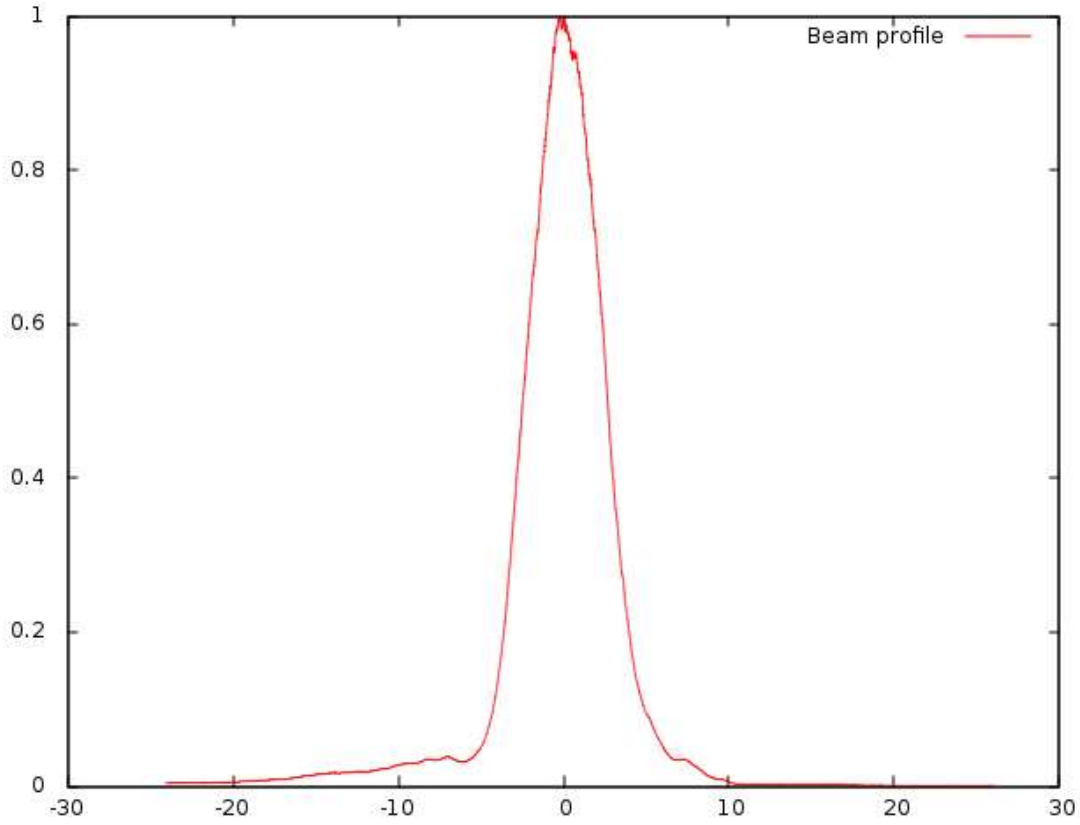

Figure 2: *Beam profile*
Horizontal axis is the azimuth beam angle in degrees, vertical scale is receive power In arbitrary units

This curve has a full width half maximum of 5.1° which is fairly close to the theoretical value. It has to be noted that the Sun is not a point source, but the impact of its extended size on the beam pattern measurement is fairly small (<0.1°) so it has been neglected here.
Some side lobes can be seen, and the pattern is somewhat asymmetrical but considered to be still quite good.
Another representation of the same data is shown in fig. 3, which is a plot in a logarithmic scale with polar coordinates.

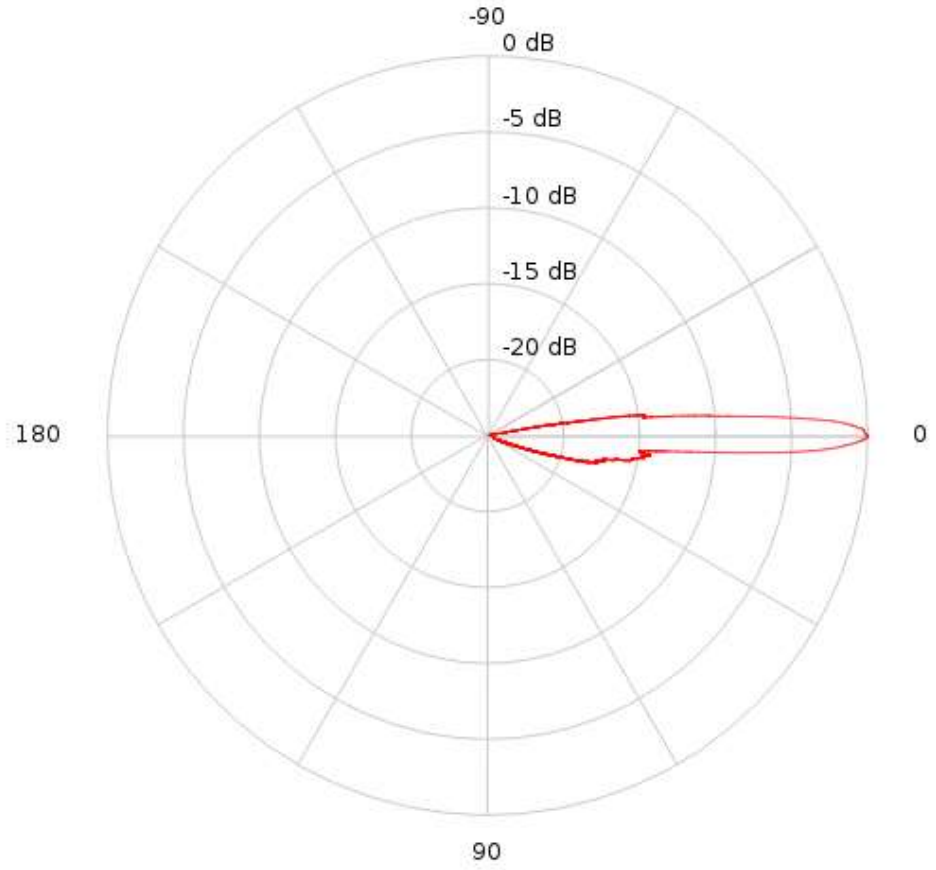

Figure 3: *Beam profile in polar coordinates*

3.2. System temperature

System temperature via Y-Method

In the radio regime the energy B received from a blackbody radiator increases linearly with the temperature T according to the Raleigh-Jeans law,

$$B_\nu(T) = \frac{2kT\nu^2}{c^2} \qquad (2)$$

where k is the Boltzmann constant, T the temperature, c the speed of light, and ν the frequency.

An ideal telescope would not show any signal if it were pointed at an extremely cold position (close to T=0). In reality there is some residual noise signal originating from the receiver itself and other imperfections. Therefore, even if the sky temperature is 0 K there is some signal which can be described by an equivalent temperature (i.e. the signal corresponds to a signal which would be experienced by an ideal telescope at this temperature), see fig. 4.
The is called the system temperature.

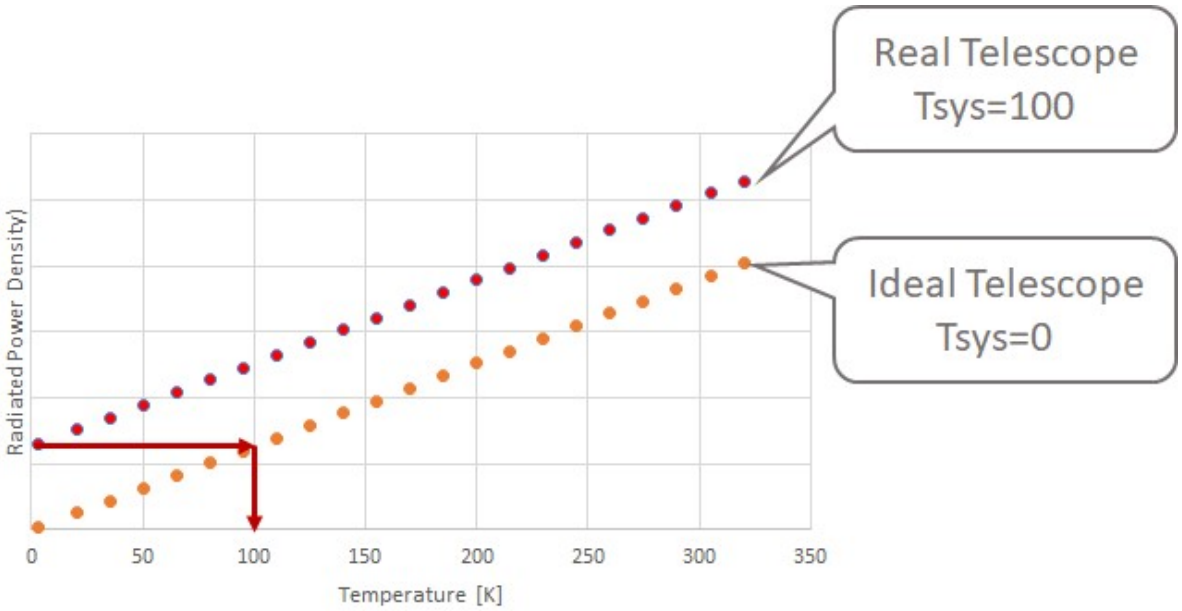

Figure 4: *Signal vs. temperature for ideal and real telescopes*

Since there is a linear relationship between signal and temperature, the system temperature can be determined by measuring the signal at two different temperatures, T_{hot} and T_{cold}. This is called the Y-Method where the system temperature T_{sys} is given by:

$$T_{sys} = \frac{T_{hot} - Y \cdot T_{cold}}{Y - 1} \tag{3}$$

with

$$Y = \frac{S_{ho}}{S_{cold}} \tag{4}$$

where S_{hot} is the signal measured at the "hot" position and S_{cold} is the signal measured at the "cold" position.
A convenient way to determine the system temperature using this method is by pointing the telescope at trees for the "hot" measurement and at the celestial pole (RA 0h, Dec 90°) for the "cold" measurement. Trees are a good approximation for a blackbody radiator and therefore the ambient temperature can be used for T_{hot}. The temperature at the celestial pole is about 10K at 1420 MHz.

Applying this methodology to our 3-m telescope gave us S_{hot} = 1606 and S_{cold} = 462 (in arbitrary units) with 275 K ambient and 10 K cold temperature. Then Y is 3.48. This results in 97 K system temperature as per equation (3). This is for an elevation of 50° as the celestial pole is at this elevation at our latitude.

System temperature via S7 calibration location
There is another nice method to determine the system temperature of a telescope operating at 21-cm wavelength. This is based on the radiometer equation:

$$\sigma_{rms} = \frac{T_{sys}}{\sqrt{\Delta\nu \cdot t}} \tag{5}$$

Rearranging this equation gives:

$$T_{sys} = \sigma_{rms}\sqrt{\Delta\nu \cdot t} \qquad (6)$$

σ_{rms} is the rms noise of the signal, $\Delta\nu$ the measurement bandwidth (per spectral channel) and t the measurement time. If the rms noise can be determined as an absolute temperature, the system temperature can be calculated. This requires an intensity calibration of the telescope.
Fortunately, there are several very well measured locations in the sky where the brightness temperature of the hydrogen line is known with high precision [1]. One of these locations is "S7" at galactic longitude 131°, galactic latitude -1°. The specific characteristic of this location is that the hydrogen distribution varies only very little over a larger region. This allows to calibrate telescopes with various beam widths. However, this is no longer quite true for larger beam widths. For a small telescope with a diameter of 3 meter and, as in our case, 5.1° beam width, the exact spectrum needs to be calculated from the original survey data. This can conveniently be done by using the tool on the website of the Argelander Institute of the University of Bonn [2].
Such a synthesised spectrum is shown below in fig. 5.

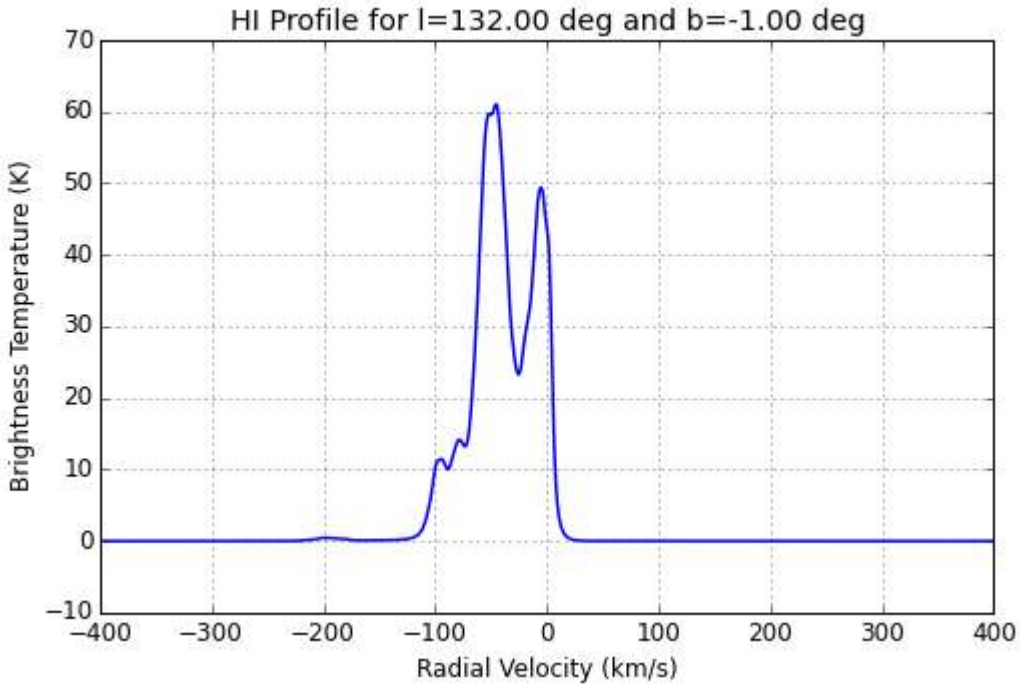

Figure 5: *Synthesized spectrum for the S7 location and 5.1° beam width*

The maximum brightness temperature is 61 K. This can now be used to calibrate the own measurement.

An observation of the S7 region with our 3-m dish provided the spectrum as shown below in fig. 6. Velocities given in this spectrum (and all spectra throughout this document) are corrected to the local standard of rest (VLSR).

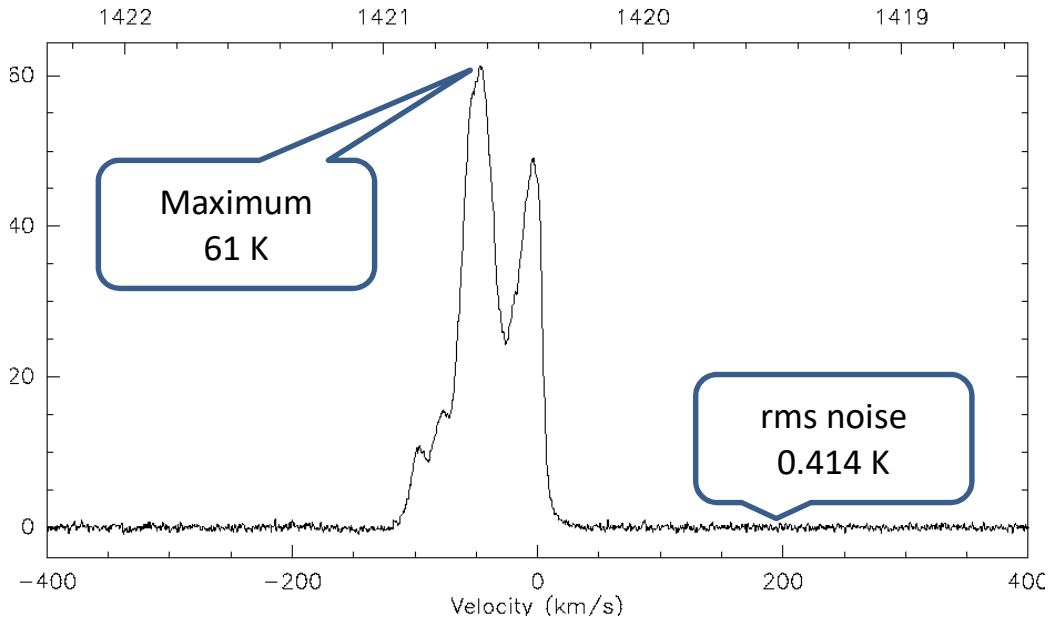

Figure 6: *Observed spectrum at the S7 location*
Vertical scale is brightness temperature in K
Upper horizontal scale is in MHz, lower horizontal scale is the VLSR corrected velocity

The vertical scale has been adjusted so that the maximum matches 61 K. Then the rms floor can be determined. In this case it has been 0.414 K. Since the integration time has been 20 seconds, and the channel bandwidth has been set to 2441 Hz, the system temperature can be calculated as:

$$T_{sys} = 0.414K\sqrt{2441 \cdot 20} = 91K \qquad (6)$$

This is in reasonable agreement with the system temperature obtained by the hot/cold method. In order to be comparable, this has also been measured at 50° elevation.

Using the same elevation for the comparison of the two methods is important, as the system temperature shows a significant dependency on the elevation. The benefit of using the S7 calibration location is that this can be measured as the location on the sky varies in elevation over time. Fig. 7 below shows this dependency. The strong increase in system temperature at 35° elevation is an effect of trees getting already partially in the line of sight of the telescope. At 30° the trees already cover the source. S7 reaches its maximum elevation at about 80° at our location.

Besides the specific effect at 35° and below due to vegetation, the overall significant variance in system temperature indicates that there is a substantial pickup of thermal background. This may be caused by the fact that the telescope is mounted close to the ground but other factors may play a role as well. Further analysis is required here.

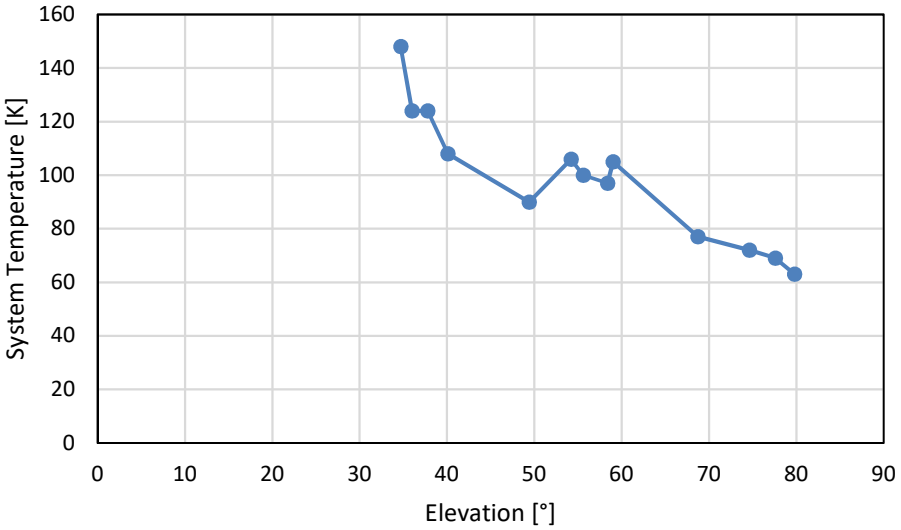

Figure 7: *System temperature at different elevations*

3.3. Forward gain

The forward gain of a radio telescope is defined as the change in antenna temperature per flux density. It is expressed in K/Jy. In order to determine this, one needs to have a known astronomical source with a defined flux density. For a small telescope, the most convenient source is the Sun. The flux density of the Sun at 1405 MHz is monitored and reported on a daily basis by the Australian Bureau of Meteorology from their Learmonth observatory [3].
On the day when we determined the forward gain, the increase in signal when pointing to the Sun was a factor of 8. The flux from the Sun was 46 solar flux units, which is 460,000 Jy.
As determined by the Y-Factor method, the increase in signal is a factor 3.48 for an increase in temperature of 265 K. Therefore, the Sun gives a rise of 609 K in antenna temperature.
This then gives a forward gain of 0.0013 K/Jy.

3.4. System equivalent flux density (SEFD)

The SEFD is often quoted as a measure for the sensitivity of a telescope. It is defined as the flux of a source which would give the same signal as the background signal due to the system temperature. The average of our two methods to determine the system temperature is 94 K at 50° elevation. Hence, the SEFD is 94/0.0013 Jy which is about 72.307 Jy at this elevation.

3.5. Aperture efficiency

From the numbers derived so far, the aperture efficiency can be calculated. The aperture efficiency is defined as the percentage of the radiation captured by the antenna aperture which is actually received. It can be calculated from

$$\eta = \frac{2kT_a}{A \cdot F} \qquad (7)$$

Where k is the Boltzmann constant, T_a the antenna temperature, A the area of the dish and F the source flux. Inserting 609 K as the antenna temperature for the Sun, 460,000 Jy as the solar flux density and 7m^2 as the antenna area yields an aperture efficiency of 52%.

3.6. Summary and assessment

Parameter	Value @ 1420 MHz
3 dB Beam Width	5.1°
System Temperature @ 50° Elevation	94 K
Forward Gain	0.0013 K/Jy
SEFD @ 50° Elevation	72,307 Jy
Aperture Efficiency	52%

Compared with expectations, the parameters are deemed reasonable. There is certainly some room for improvement, but as the subsequent observations will show it serves its purpose.

4. Spectral Observations

The prime objective of this telescope is to observe the hydrogen emission from the Milky Way and to use these observations in various lab courses for students from university and schools.
Therefore, good performance in this application was important.

4.1. Hydrogen emission: Sample spectrum

A sample spectrum from the hydrogen emission in the galactic plane is shown in fig. 8 below. This spectrum is taken at 80° of galactic longitude and 0° of galactic latitude. At this location, the emission is quite bright with almost 100 K brightness temperature. The integration time was 20 seconds and the spectral resolution was 3.662 KHz/channel. Calibration of this measurement was performed via observation of the S7 reference region.

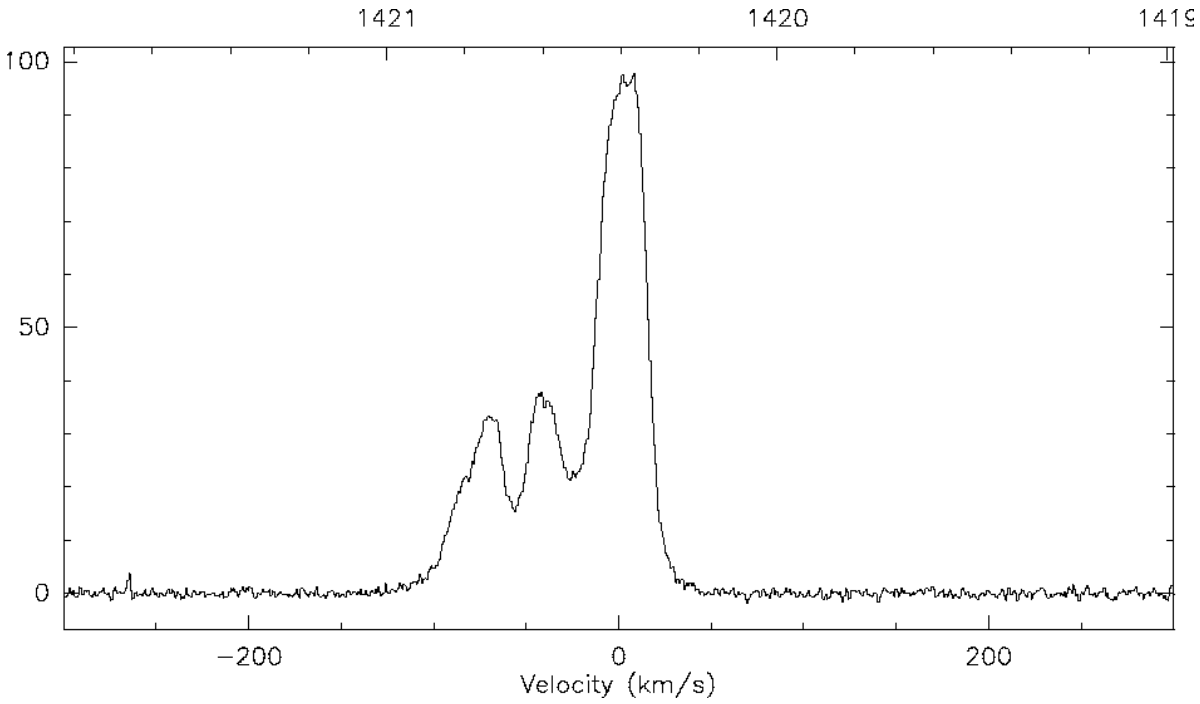

Figure 8: *Hydrogen emission spectrum at l=80°, b=0°*
Vertical scale is brightness temperature in K
Upper horizontal scale is in MHz, lower horizontal scale is the VLSR corrected velocity

4.2. Hydrogen emission: Scan of the galactic plane

One of the tests was to scan the galactic plane and to take spectra at small increments of 0.5° of the galactic longitude. The longitudes from close to 0° up to about 240° are accessible from the geographical location of our 3-m telescope.
The result is shown as a heat map in fig. 9 below.

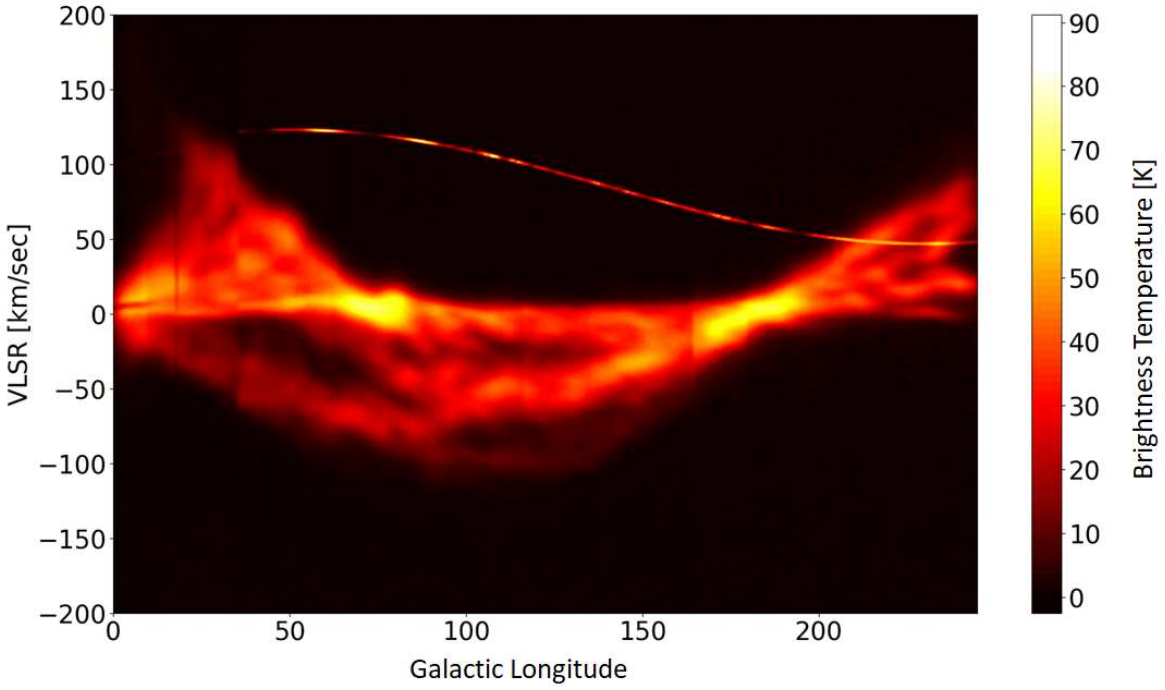

Figure 9: *Scan of the galactic plane (Galactic latitude 0)*

The velocities are given in the local standard of rest reference frame. Calibration of the intensity has been performed by measuring the spectrum at the S7 location. This should be taken with some caution, though, as the measurement took quite some time and the gain might have changed a bit during this time.
There is a spurious line through almost all of the scan due to some RFI. This line is at a fixed frequency but appears at different velocities due to the correction to the local standard of rest.

4.3. High velocity clouds

High velocity clouds (HVCs) are clouds of hydrogen which are observed at various places in the sky. These are patches of hydrogen which have a distinct different velocity compared to the hydrogen in the arms of the Milky Way. These patches are believed to be falling into the galactic plane, attracted by the gravitation of the Milky Way. The origin of these clouds has not been finally determined. The most common theories are that these are intergalactic clouds which have been collected by the Milky Way, or that the hydrogen has been ejected by a supernova explosion and is now falling back. These clouds are substantially weaker than the “ordinary” hydrogen emission but can be detected with the 3-m dish. The spectrum in fig. 10 below shows the emission of the so-called H-complex with a blue shifted velocity of 200 km/s. The strong signal in the middle is from the hydrogen in the galactic plane. The H-complex is located at about 150° galactic longitude and 35° galactic latitude.

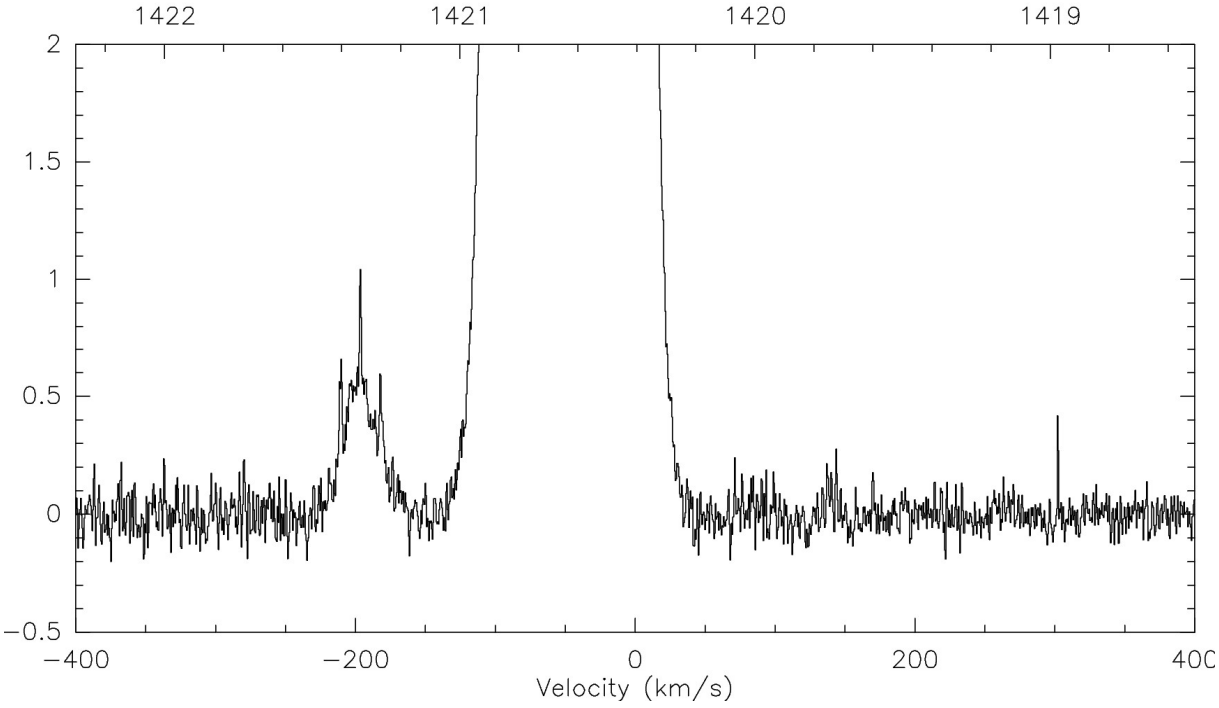

Figure 10: *High velocity cloud at -200 km/s*
Vertical scale is the brightness temperature in K,
upper horizontal scale is in MHz, lower horizontal scale is the VLSR corrected velocity

The integration time for this observation was 30 minutes.

4.4. Circumstellar OH masers

Circumstellar OH Masers are bright sources emitting at a hyperfine structure transition of the Hydroxyl radical at 1612 MHz. A comprehensive description of these types of astronomical radio sources can be found at our website [4] where we have described the observation of OH masers with our 25-m dish.
The feed horn of the 3-m dish had been designed so that the 1612 MHz range is supported at least to some extent. We were hoping that the strongest OH masers might be observable with the 3-m dish. Indeed, the attempt to detect the OH maser around the Red Supergiant Star NML Cyg was successful. The spectrum achieved with 2.5 hours integration time is shown below in fig. 11. The spectrum recorded with the 3-m dish is the black line. The red line is a spectrum recorded with our 25-m dish for the purpose of comparison and verification.

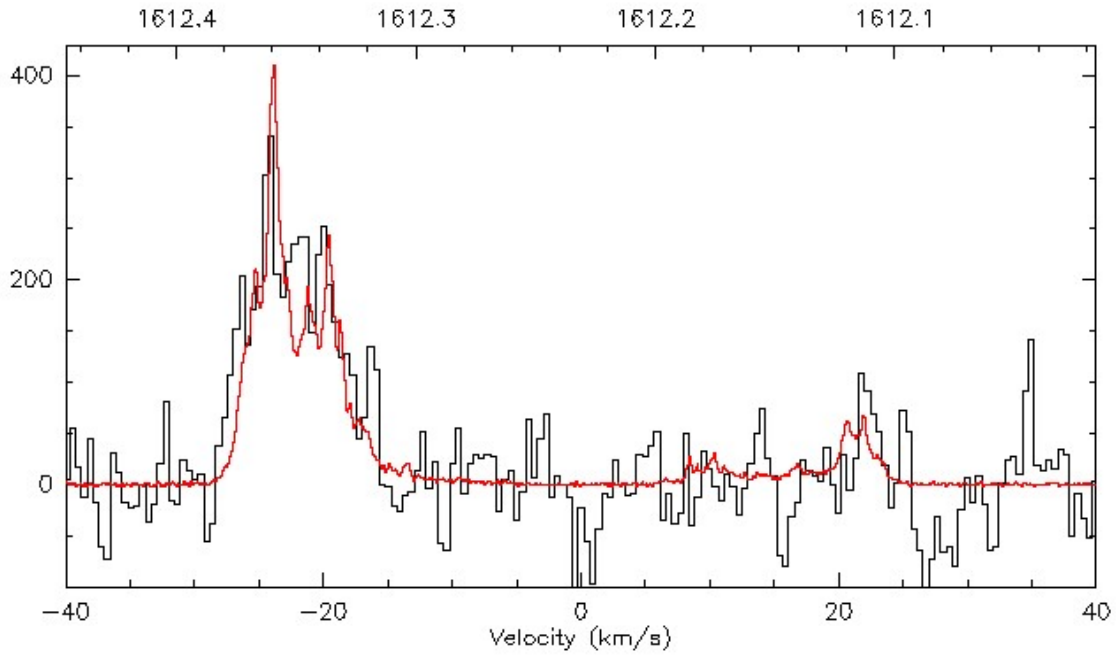

Figure 11: *OH maser spectrum of NML Cyg*
Vertical scale is in Jansky, upper horizontal scale is in MHz,
lower horizontal scale is the VLSR corrected velocity

The 3-m dish is not independently calibrated at 1612 MHz. We used the calibrated measurement from the 25-m dish to scale the 3-m dish data. Scaling was done so that the integrated flux density (Jy*km/s) of the 3-m observation was equal to the integrated flux density of the 25-m measurement.

5. Continuum Observations

The observation of continuum sources, i.e. sources which emit a very broad spectrum are a bit tricky and require careful consideration in order not to be misled by artefacts.
The very fundamental limit of the source flux density which can be observed is governed by the radiometer equation (5). For 94 K system temperature, 10 MHz of bandwidth and 1 second integration time, a SNR of 1 is achieved with 0.03 K increase of the antenna temperature. Given our forward gain of 0.0013 K/Jy this translates to 23 Jy as the minimum detectable flux density. This sounds very interesting as CAS A has a flux of 1670 Jy, so a signal very well above the noise floor can be expected.
As usual, things are a bit more complex in the real world ☹.
Applying the radiometer equation implies that there are no factors influencing the measurement other than a constant background noise. In reality, there are additional effects. There is a variation of the receiver background noise due to fluctuations in gain, in particular due to temperature variations. Then, in order to detect a source, one needs to compare the signal at the “on” position with the signal at the “off” position. This requires a movement of the telescope. Such a movement, however, will change the thermal background picked up by the telescope quite a bit. If we look at the dependency of the system temperature on the elevation in our case, it becomes obvious that even small movements can create a signal difference far larger than the signal increase from weak sources.

Therefore, a careful observation strategy has to be applied for successful detection of continuum sources. The aim of such a strategy is to minimize the background effects mentioned. Where such effects are unavoidable, the data needs to be interpreted carefully.

5.1. Observation strategies

There are two basic strategies, transit scans and active scans. Both have their advantages and disadvantages:

Transit scans:
A transit scan is an observation where the telescope is kept stationary and the transit of the source is achieved due to the rotation of the earth. The telescope is pointed to a position in the sky where the source will be in the future and then data is recorded while the source is passing through the beam. The obvious advantage of this method is that there is in principle no change in terrestrial background signal. The disadvantage lies in the long duration of such a scan. At 5° beam width, one needs to have a very significant time offset to ensure that the measurements starts with the source well outside the beam. The measurement then has to continue until the source is well outside the beam again. This will typically be a two-hour exercise. During this time, many things can happen. Obviously, the outside temperature can change which will influence the signal. Other gain drifts are also likely to happen. Furthermore, there can be RFI coming up or disappearing which may even invalidate the measurement.

Active scans:
An active scan can be performed much quicker than the transit scan. The advantage therefore is that temperature variations can be small or negligible. Changing the terrestrial background due to the motion, though, is the culprit. One needs to minimize this effect as far as possible.
Due to the strong variation of system temperature with elevation it is not advisable to do a scan in elevation. The better method is to change the azimuth. But even then, changes in terrestrial background will be observed. When the azimuth only is changed, both right-ascension and declination are changed during the scan. This makes it more difficult to identify the sky position of the signal maximum and compare this with the expected position.
Another option is to scan in either right-ascension or declination. This will of course change both azimuth in elevation. If a right ascension scan, however, is performed at a time when the source is culminating the variation in elevation will be small. At times when the source is at it's midpoint between its highest and lowest point, then a scan in declination will minimize movement in elevation. Yet another scan strategy can be to scan in galactic coordinates.

On target/Off target
Frequently, a method is proposed where the position is switched between on target and off target. We did not find this method to be well suited for a small telescope. It becomes undistinguishable whether the change in intensity is due to a source or due to the variation in terrestrial background. This method is better suited for large telescopes with their small opening angles where the difference between the on and off position can be kept much smaller.

Continuum observations are presented below. The centre frequency of the measurement was 1407 MHz with a bandwidth of 10 MHz. This prevents any emissions from the hydrogen line affecting the result. The different scan strategies are also demonstrated.

5.2. Specific Targets

Cassiopeia A

Besides the Sun, the Supernova Remnant Cassiopeia A (CAS A) is the brightest continuum source in the radio sky at 1400 MHz Therefore, it is the most promising target when trying continuum observations. CAS A has a flux density of about 1670 Jy (measured in year 2017 with our 25-m dish). The increase in antenna temperature which can be expected from this source therefore is about 2.3 K at our forward gain.

First, a transit scan was performed. Furthermore, in order to verify the result, the telescope has been kept in position and the transit of CAS A has also been observed on the subsequent day.

Fig. 12 below shows the result of this experiment. The transit can clearly be seen on both days at the expected right ascension.

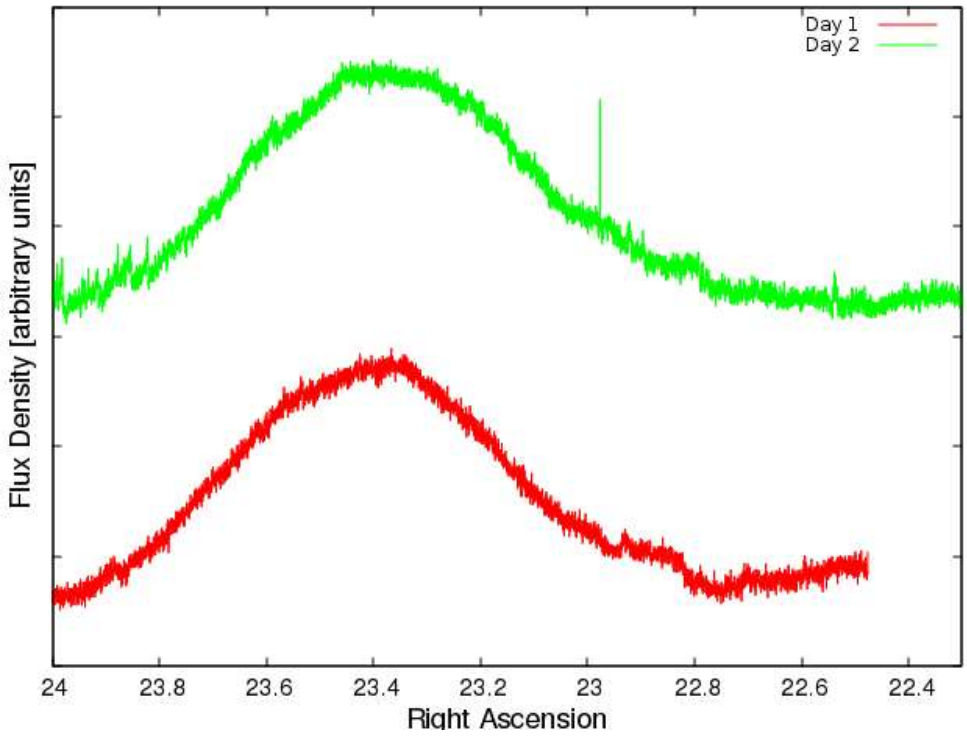

Figure 12: *Transit Scan of Cassiopeia A, signal from two subsequent days*

The vertical displacement of the two curves is due to some drift in the receiving chain over the 24 hours of the observation.

A good result was also achieved with an active scan over right ascension. This was when CAS A was in a favourable position close to its culmination. This minimized the effect of variation in system temperature with the change in elevation.

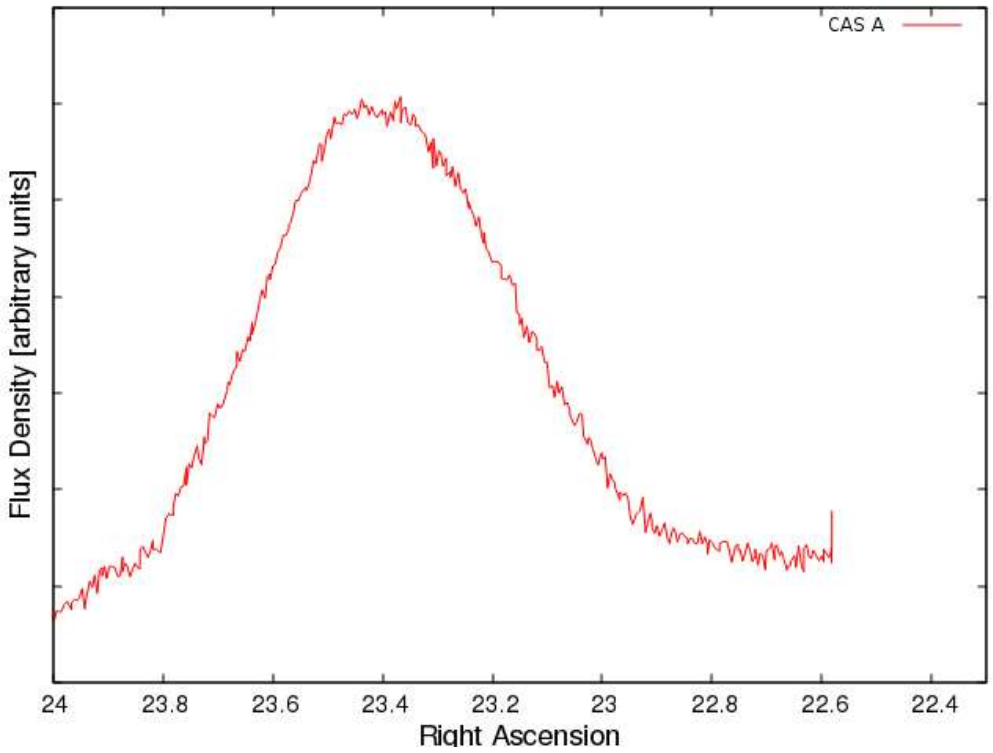

Figure 13: *Active Scan of Cassiopeia A*

Cygnus complex

A close runner-up to CAS A in terms of flux density is Cygnus A (CYG A) with 1550 Jy. CYG A is a radio galaxy at a distance of 750 million light years. Given the result with CAS A it was expected that CYG A would be visible as well.

The transit scan of CYG ended with a surprise: This signal increased as expected at the correct right ascension but continued to increase even when CYG A was expected to move out of the beam. Repeated transit gave the same result. The reason for this behaviour turned out to be that beside CYG A there is the complex Cygnus X. This is an area with several star forming regions which are also continuum emitters. The limited spatial resolution of a 3-m dish leads to a confusion between CYG A and CYG X; they become mostly indistinguishable. Furthermore, all the sources within CYG X contribute to the signal so the overall brightness is quite large. As a consequence, the total Cygnus complex becomes brighter than CAS A when observed with a 3-m telescope.

The plot of the transit scan of the Cygnus complex is shown in fig. 13. For comparison, the same transit with a 25-m dish is shown (green line) to demonstrate the neighbourhood of CYG A and CYG X. Since CYG X is also extended in declination, this becomes the dominant source for the 3-m dish. CYG A only manifests itself as a “bump” in the curve at RA=20.

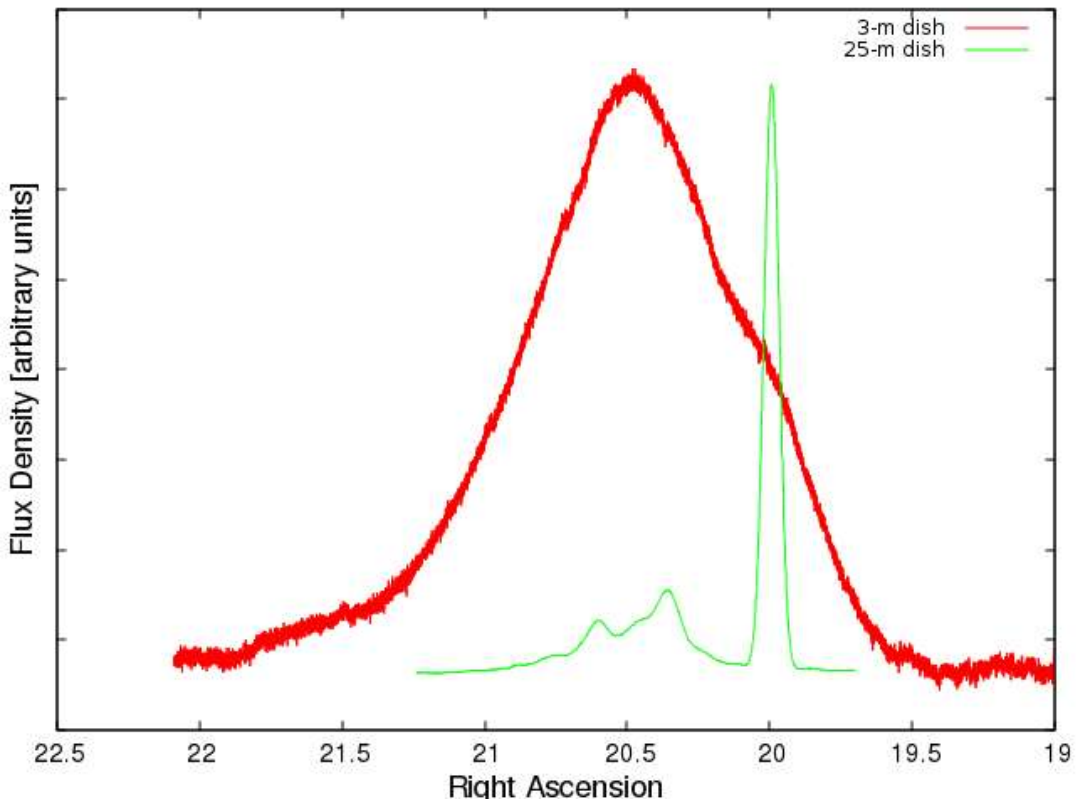

Figure 14: *Transit Scan of Cygnus Complex*
Scan with 25-m dish (green line) shown for comparison, vertical not to scale

The geometry of the scan and the effect of the large beam size is also depicted below in fig. 15 where a contour map based on the 1420 MHz all sky survey data by Reich et. al. [5],[6] is shown beside the scans.

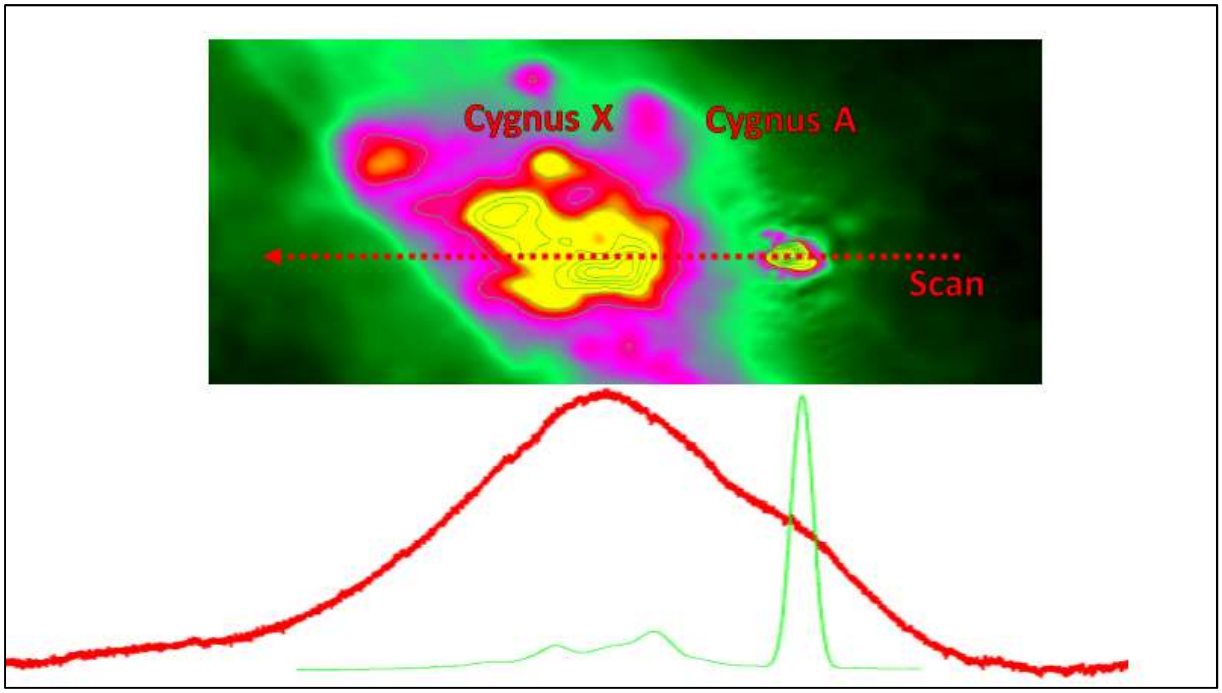

Figure 15: *Contour map of the Cygnus complex and the two scans in comparison*

The contour map has been prepared by downloading data from the survey tool of the Max-Planck Institute for Radio Astronomy [7] and subsequent processing of the FITS file.

Also, for this source an active scan over right ascension was tried when it was close to culmination. The result is shown in fig. 16.

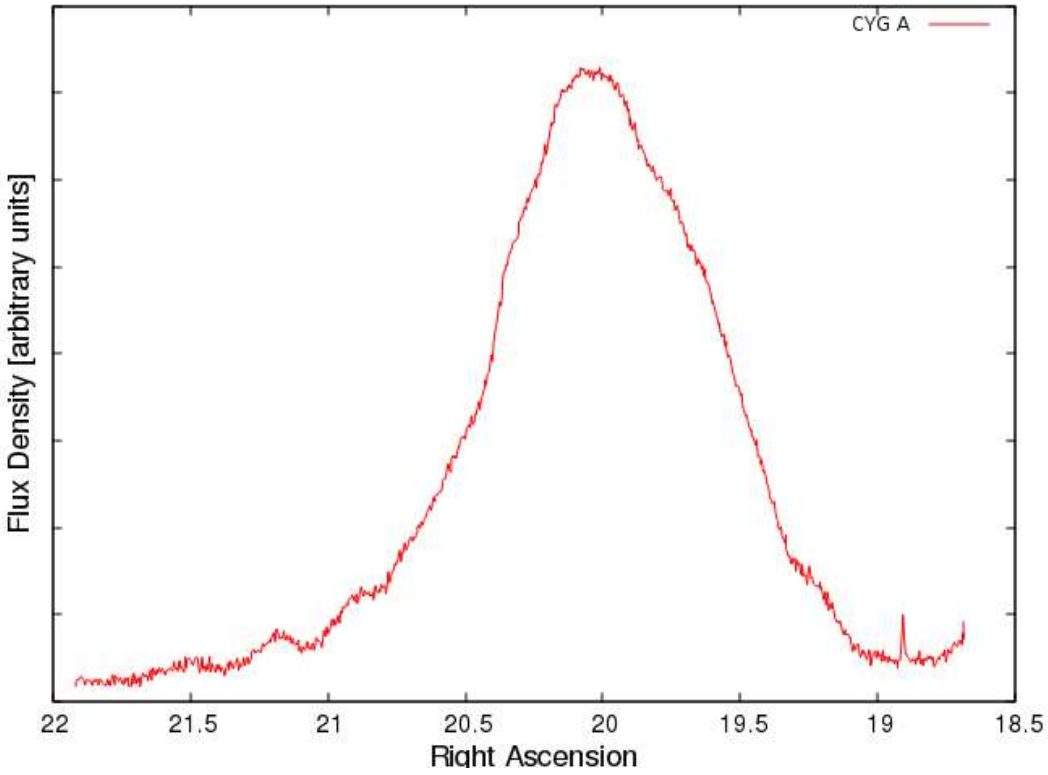

Figure 16: *Active Scan of Cygnus A*

Crab Nebula (M1, Taurus A)

Another strong source is the Crab nebula, a supernova remnant. Also, for this source one can observe a confusion with a neighbouring source. In this case the distance is somewhat larger and two distinct peaks can be identified as shown in fig. 17.

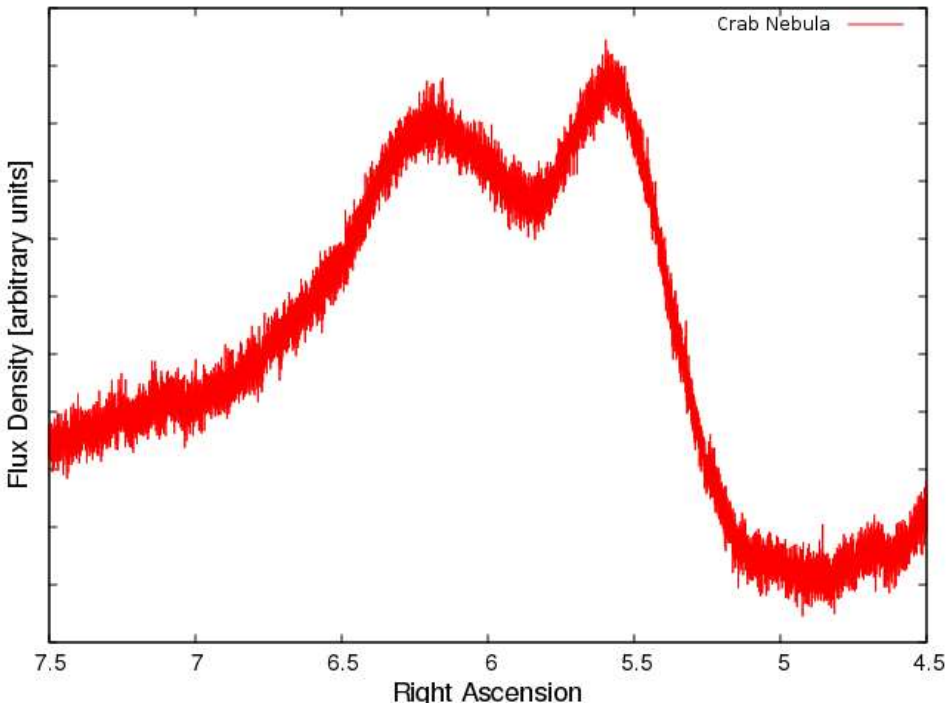

Figure 17: *Transit Scan of the Crab Nebula*

We have identified the neighbouring source as another supernova remnant, 3C157 (IC443) at RA 06:18:02.7, Dec +22:39:36. A map of the area created from survey data is shown below in fig. 18.

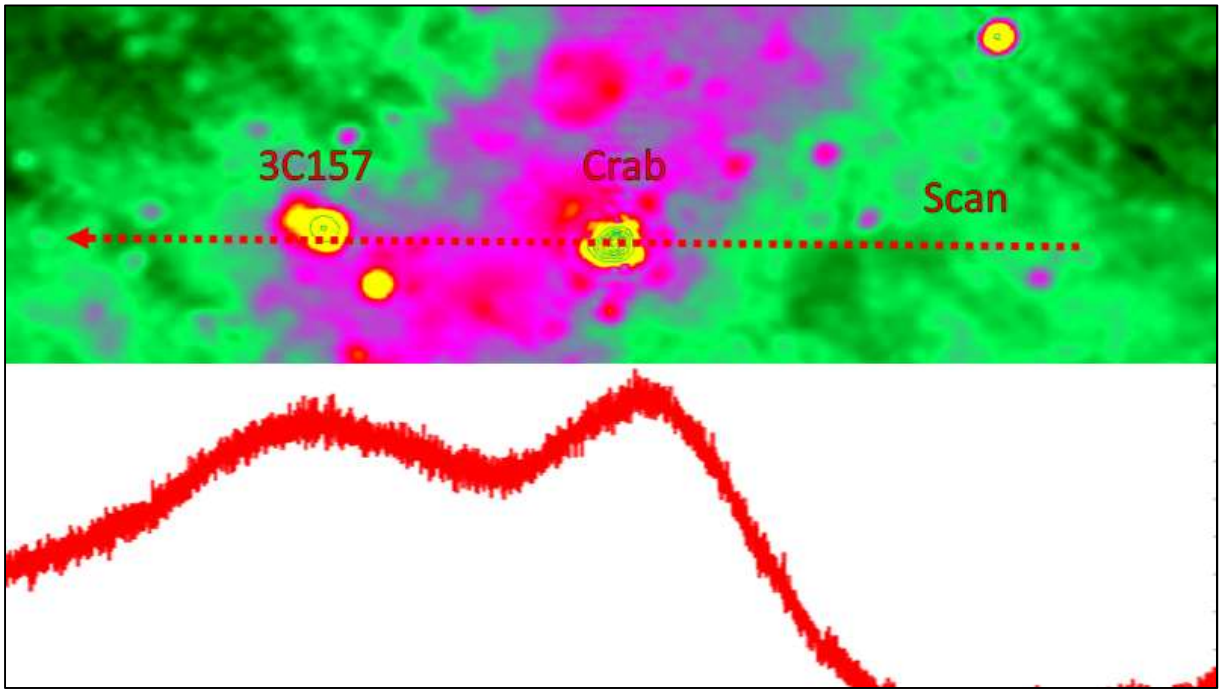

Figure 18: *Contour map of the Crab Nebula and 3C157 region and scan in comparison*

Orion Nebula (M 42)

This Orion nebula is a star forming region in our Milky Way and can be detected via a transit scan.

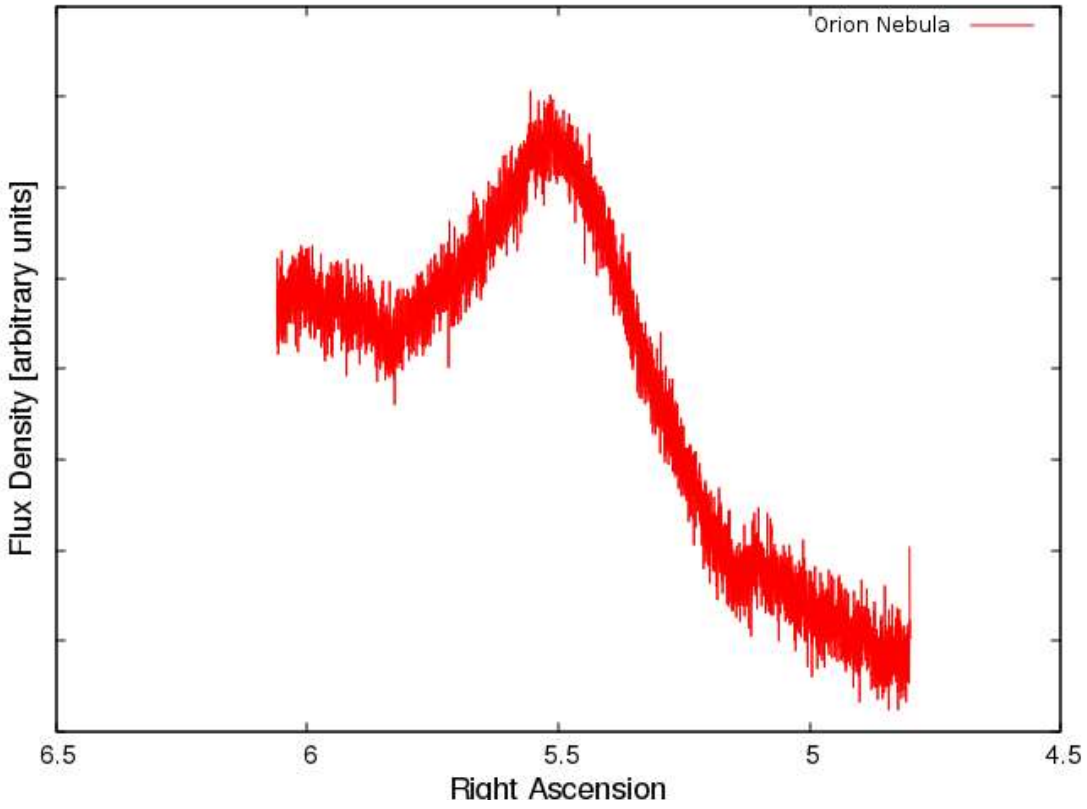

Figure 19: *Transit Scan of the Orion Nebula*

A significant drift can be seen in the background signal during the transit scan but the signal from Orion can still be identified clearly.

Virgo A (M 87)

This source has become very famous as the first radio galaxy where the black hole in the centre has been depicted by the Event Horizon Telescope [8]. Since the flux from this source at 1405 MHz is reported to be 213 Jy this is expected to be detectable with a 3-m dish. Indeed, this was possible with a drift scan (fig.20). There is a substantial drift of the background. Only the repeatability of this signal confirmed that this is actually a valid observation.

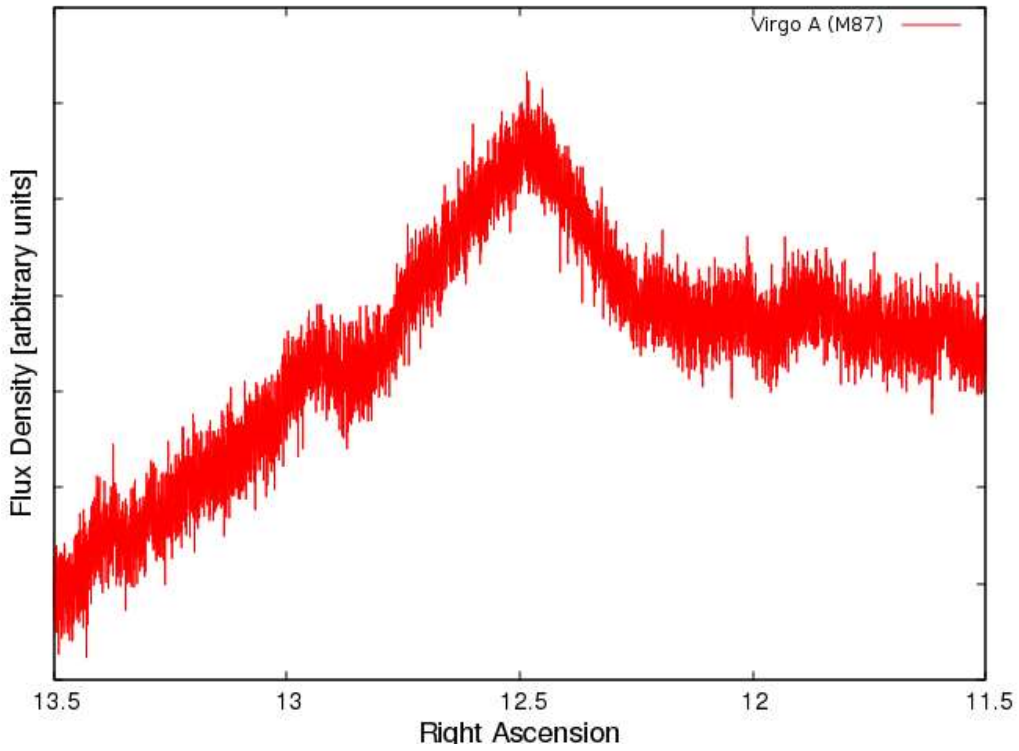

Figure 20: *Transit Scan of the Virgo A (M87)*

5.3. Synchrotron radiation from the galactic plane

Besides specific, strong targets like radio galaxies, star forming regions and supernova remnants there is a fairly strong continuum emission from the galactic plane. It is particularly intense in the region around the galactic centre. This was investigated by doing a number of active scans in galactic coordinates. This was done by scanning from approx. -12° galactic latitude to +12° galactic latitude for a number of galactic longitudes. It would have been desirable to start at the galactic centre. However, at our geographic latitude the galactic centre is quite low on the horizon and for our 3-m dish it is already behind trees. Also, for lower galactic longitude there is substantial impact due to thermal radiation from the vegetation. Therefore, meaningful scans were possible from 15° longitude onwards. This was done with increments of 5° until the signal essentially disappeared at 55° longitude.
The scan paths are shown fig. 21. These are overlaid over a contour map of the galactic plane in that region. The projection of that map is in galactic coordinates, the data was again taken from [7].
The scan results are shown in fig. 22. In particular the scan for 15° longitude shows a significant impact from thermal pickup due to the low elevation required for the scan. Nevertheless, the peak at the galactic plane can be seen as for the other longitudes.

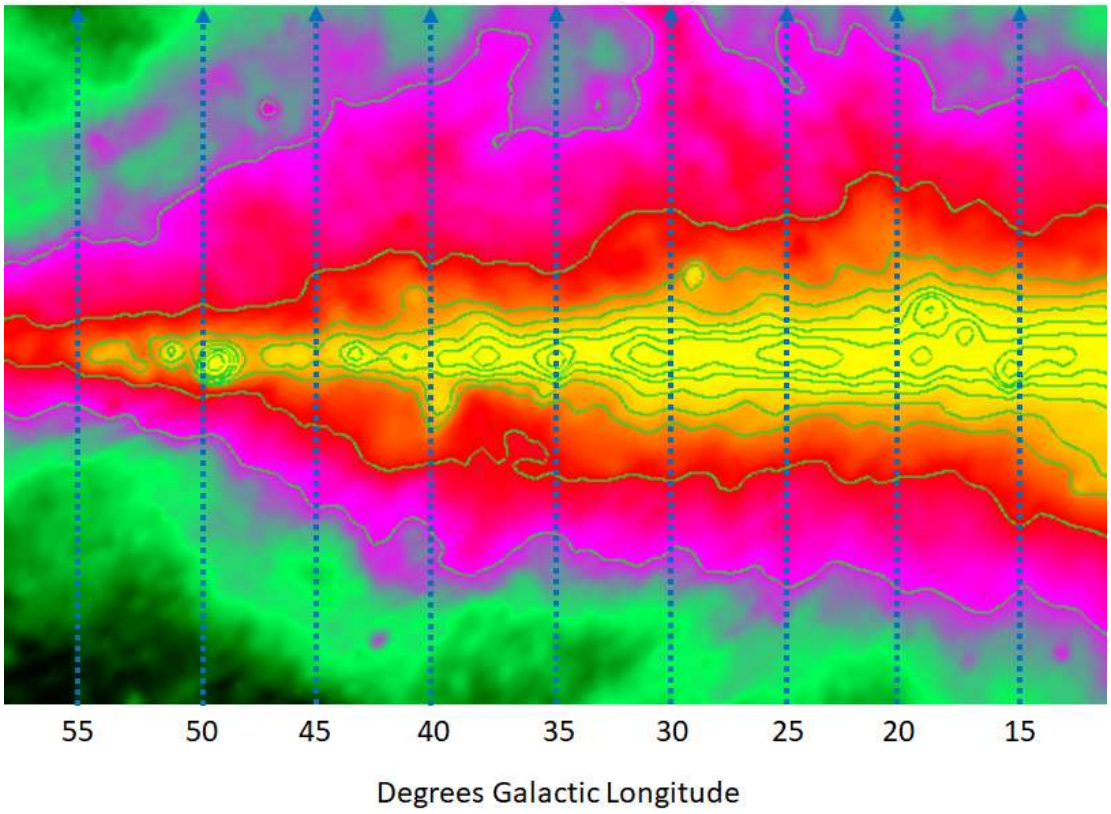

Figure 21: *Scan paths through the galactic plane*

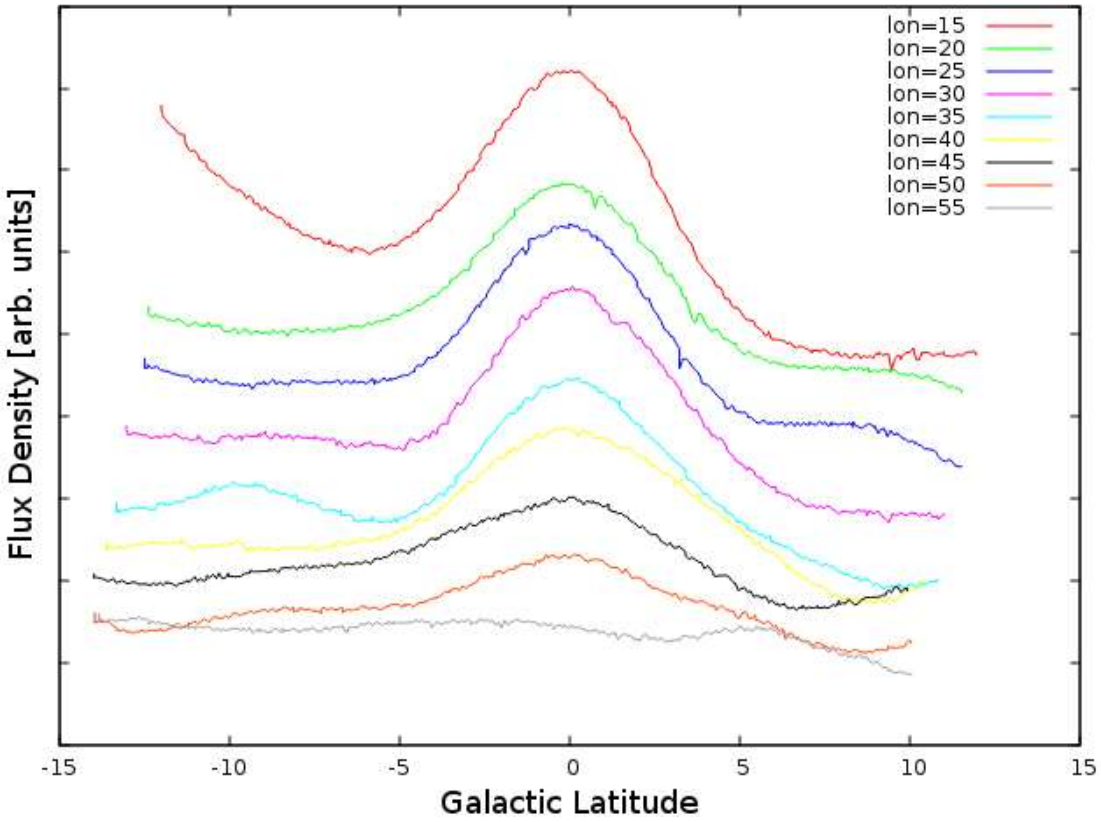

Figure 22: *Results of scans*

6. Conclusions and further work

As demonstrated by this setup, a dish with a diameter of 3 meters can be a fairly powerful instrument and allow a wide range of observations. Observing the emission of the hydrogen 21-cm line from the Milky Way is a fairly easy task with such an instrument. Even weaker emissions like the high velocity clouds can be detected. If one wishes to reach out to other wavelengths, also the strongest OH masers at 1612 MHz are within reach of such a dish.
It has successfully been demonstrated that stronger continuum source can be detected with an instrument of this size when choosing the scan strategy carefully.

Further work with this instrument will include attempts to observe the 21-cm emission from the Andromeda galaxy and the strongest pulsar, B0329+54. It has been successfully demonstrated by others that this is doable [10],[11],[12] with a dish of this size. However, further optimization may be required in order to achieve these targets.

References:

[1] P.W.M. Kalberla et. al., Brightness Temperature Calibration for 21-cm Line Observations, Astron. Astrophys. 106, 190-196 (1982)
[2] https://www.astro.uni-bonn.de/hisurvey/euhou/LABprofile/
[3] https://www.sws.bom.gov.au/Solar/3/4/2
[4] https://astropeiler.de/sites/default/files/Astropeiler_Story_5.pdf
[5] W. Reich, A radio continuum survey of the norther sky at 1420 MHz I, Astron. Astrophys. Suppl. Ser. 48, 21 9-297 (1982)
[6] P. Reich, W. Reich, A radio continuum survey of the norther sky at 1420 MHz II, Astron. Astrophys. Suppl. Ser. 63, 205-292 (1986)
[7] https://www3.mpifr-bonn.mpg.de/survey.html
[8] https://eventhorizontelescope.org/
[9] Baars et.al., The Absolute Spectrum of CAS A; An Absolute Flux Density Scale and a Set of Secondary Calibrators, Astron. Astrophysics 61, 99-106 (1977)
[10] https://f1ehn.pagesperso-orange.fr/fr/f_radioastro.htm
[11] http://neutronstar.joataman.net/sites/s5/docs/jn65tw.pdf
[12] https://www.qsl.net/oe5jfl/pulsar/pulsar_3m_dish.htm